Natively Unfolded Human Prothymosin α Adopts Partially Folded Collapsed Conformation at Acidic pH†

Vladimir N. Uversky,*,‡,§,|| Joel R. Gillespie,|| Ian S. Millett,⊥ Anna V. Khodyakova,§ Anatoly M. Vasiliev,§ Tatyana V. Chernovskaya,§ Raisa N. Vasilenko,§ Galina D. Kozlovskaya,§ Dmitry A. Dolgikh,# Anthony L. Fink,|| Sebastian Doniach,⊥ and Vyacheslav M. Abramov§

Institute for Biological Instrumentation, Russian Academy of Sciences, 142292 Pushchino, Moscow Region, Russia, Institute of Immunological Engineering, 142380 Lyubuchany, Moscow Region, Russia, Department of Chemistry and Biochemistry, University of California, Santa Cruz, California 95064, Departments of Physics and Chemistry, Stanford University, Stanford, California 94305, and Shemyakin and Ovchinnikov Institute of Bioorganic Chemistry, Russian Academy of Sciences, 117871 Moscow, Russia

Received March 31, 1999; Revised Manuscript Received September 21, 1999

ABSTRACT: Prothymosin α has previously been shown to be unfolded at neutral pH, thus belonging to a growing family of "natively unfolded" proteins. The structural properties and conformational stability of recombinant human prothymosin α were characterized at neutral and acidic pH by gel filtration, SAXS, circular dichroism, ANS fluorescence, ^{1}H NMR, and resistance to urea-induced unfolding. Interestingly, prothymosin α underwent a cooperative transition from the unfolded state into a partially folded conformation on lowering the pH. This conformation of prothymosin α is a compact denatured state, with structural properties different from those of the molten globule. The formation of α-helical structure by the glutamic acid-rich elements of the protein accompanied by the partial hydrophobic collapse is expected at lower pH due to the neutralization of the negatively charged residues. It is possible that such conformational changes may be associated with the protein function.

Prothymosin α (ProTα)[1] is an acidic nuclear protein with wide tissue distribution (*1*, *2*), initially isolated from the rat thymus (*3*). Although the thymus is the richest source of ProTα, the ProTα gene was shown to be expressed in a wide variety of tissues (*4*). Despite the exact function of ProTα remaining unknown, this protein is often considered as a thymic hormone with immunostimulating properties or as a precursor of thymosin α1, a hormone-like peptide (28 amino acid residues) derived from the amino terminus of ProTα. Thymosin α1, as with other peptides isolated from thymus gland, can restore relevant parameters of the immune response in thymus-deprived animals and in vitro systems (*5*) as well as immunodeficient patients (*6*, *7*). Interestingly, ProTα is even more potent than thymosin α1 in the protection of animals against opportunistic infection (*8*). ProTα promotes maturation and differentiation of lymphoid cells, regulates production of interleukin-2, and enhances expression of interleukin-2 receptors in human T-lymphocytes (*9*, *10*) as well as promotion of murine antitumor activity (*11*).

On the other hand, there is some evidence that ProTα is associated with cell proliferation. The ProTα gene is activated by the *c*-myc protein (*12*). Increased levels of ProTα are observed in cancer tissue (*13*), and the division of myeloma cells can be inhibited by treatment with ProTα antisense oligomers (*14*).

The presence of a nuclear-targeting sequence near the carboxy terminus of the ProTα molecule indicates that it is capable of accumulation in the nucleus (*15*, *16*), and indeed it has been shown to interact with the histone protein H1 (*17*). It has been suggested that ProTα may be required to open chromatin (*13*).

Interestingly, of the 109 amino acid residues of ProTα, roughly half are aspartic and glutamic acids; there are no aromatic residues and no cysteines (*18*). According to NMR, CD, SAXS, static, and dynamic light scattering data, purified ProTα is in a random coil conformation under physiological conditions (*16*, *18*, *19*). Some increase in the ordered secondary structure content has been reported for the protein at acidic pH (*16*, *18*).

Recently, it has been shown that under equilibrium conditions proteins can adopt at least two different compact denatured states (partially folded conformations): the molten globule and the premolten globule (*20*−*29*). It has been

† This work was supported in part by Grants 97-04-49227 and 96-15-98008 from the Russian Foundation for Basic Research, by Grants 403 and 463 from the International Science and Technology Center (US and EU are the financial parties), and by NATO Collaborative Linkage Grant LST.CLG 975190.

* Corresponding author. Tel.: 831-459-2915. Fax: 831-459-2935. E-mail: uversky@hydrogen.ucsc.edu.

‡ Institute for Biological Instrumentation.

§ Institute of Immunological Engineering.

|| University of California.

⊥ Stanford University.

Shemyakin and Ovchinnikov Institute of Bioorganic Chemistry.

[1] Abbreviations: ProTα, prothymosin α; GdmCl, guanidinium hydrochloride; CD, circular dichroism; SDS−PAGE, sodium dodecyl sulfate−polyacrylamide gel electrophoresis; NMR, nuclear magnetic resonance; SAXS, small-angle X-ray scattering; UV, ultra violet; ANS, 8-anilino-1-naphthalene sulfonate; R_S, Stokes radius; R_g, radius of gyration; N, native state; MG, molten globule state; PMG, premolten globule state; U, unfolded state; BSA, bovine serum albumin.

10.1021/bi990752+ CCC: $18.00
Published on Web 10/21/1999

proposed that the molten globule (*30*, *31*) as well as its precursor (*22*, *24*) may be of physiological importance. For the molten globule state, this suggestion has been successfully confirmed by several studies (see refs *31* and *32* for reviews).

In the present paper, the pH-induced changes of ProTα structure and stability were studied by a number of physicochemical methods, including circular dichroism, ANS fluorescence, gel filtration, SAXS, and ^{1}H NMR. The results indicate that a decrease in pH results in the transformation of unfolded ProTα into a partially folded conformation.

MATERIALS AND METHODS

Recombinant-Produced Protein. Human prothymosin α was produced in *Escherichia coli* as previously described (*33*). SDS−PAGE was performed according to Laemmli (*34*). The effect of recombinant ProTα on the proliferactive response was evaluated in the blast-transformation reaction. Human thymocytes were cultured in 96-well plates in RPMI medium (Gibco) containing embryonic calf serum, 5 mM HEPES, 50 unit/mL gentamycin, and 20 mM L-glutamine. To assess the reaction, 1 μCi of [^{3}H]thymidine was introduced into each well (*35*), and DNA synthesis (proliferation) was measured by [^{3}H]thymidine incorporation. *E. coli*-derived recombinant human interleukin 4 (rHuIL-4) was used for comparison in the activity measurements.

Determination of the Protein Concentration. As ProTα does not contain any aromatic amino acid residues, the usual spectroscopic measurement of the protein concentration was not possible. Instead, the concentration of ProTα was calculated from the nitrogen content determined by protein incineration on a CHN analyzer. The expected nitrogen content per protein molecule was calculated from the known amino acid sequence of ProTα.

Gel Filtration. Hydrodynamic dimensions (Stokes radius, R_S) of Protα in different conformational states were measured by gel filtration. Gel filtration measurements were carried out on a Superose 12 HR 10/30 column using a Pharmacia FPLC apparatus. A set of globular protein with known R_S values was used (*36*, *37*). The gel filtration column was calibrated in terms of $1000/V$ vs R_S dependence, where V is the elution volume of the given protein (*36*−*40*). A least-squares analysis was applied to fit the experimental data to generate the calibration curve:

$$1000/V = (0.73 \pm 0.01)R_S + (52.0 \pm 0.4) \qquad (1)$$

Hydrodynamic dimensions of native and completely unfolded globular proteins with a molecular mass of 12 kDa were calculated from empirical equations (*36*):

$$\log (R_S^N) = 0.369 \times \log (M) - 0.254 \qquad (2)$$

$$\log (R_S^U) = 0.533 \times \log (M) - 0.682 \qquad (3)$$

based on the intrinsic viscosity data (*41*). Here R_S^N and R_S^U are the Stokes radii of native (N) and completely unfolded (U) proteins, respectively.

SAXS Measurements. Small-angle X-ray scattering (SAXS) measurements were made using the SAXS instrument on Beam Line 4-2 at the Stanford Synchrotron Radiation Laboratory. Scattering patterns were recorded by a linear position-sensitive proportional counter, which was filled with an 80% Xe/20% CO_2 gas mixture. Scattering patterns were normalized by incident X-ray intensity, which was measured with a short-length ion chamber before the sample. The sample-to-detector distance was calibrated to be 230 cm using a cholesterol myristate sample. To avoid radiation damage of the sample in equilibrium and manual mix measurements, the protein solution was continuously passed through a 1.3-mm path length observation flow cell with 25-μm mica windows. Background measurements were performed before and after each protein measurement and then averaged before being used for background subtraction. All SAXS measurements were performed at 23 ± 1 °C.

Radii of gyration (R_g) were calculated according to the Guinier approximation (*42*):

$$\ln I(Q) = \ln I(0) - R_g^2 Q^2/3$$

where Q is the scattering vector given by $Q = (2\pi \sin \theta)/\lambda$ (2θ is the scattering angle and λ is the wavelength of X-ray). $I(0)$, the forward scattering amplitude, is proportional to $n\rho_c^2V^2$ where n is the number of scatters (protein molecules) in solution; ρ_c is the electron density difference between the scatter and the solvent; and V is the volume of the scatter (*42*).

Spectroscopic Measurements. Circular dichroism measurements were carried out using a Jasco-600 spectropolarimeter (Jasco, Japan) equipped with a temperature-controlled cell holder. The cell path length was 0.148 mm, and protein concentration was 0.6 mg/mL.

ANS fluorescence was measured by an Aminco SPF-1000 CS spectrofluorometer with excitation at 360 nm and a protein concentration of 0.1 mg/mL. The ANS concentration was 25 μM.

^{1}H NMR spectra were collected on a Varian Unity+ 500 MHz spectrometer equipped with ultrashims. All data were collected at 25 °C, and presaturation was used for water suppression. Proton spectra were collected on a 0.5 mM sample of prothymosin α in water containing 10% D_2O. The pH of the sample was adjusted using NaOH or HCl and was uncorrected for deuterium isotope effect. NOESY spectra were collected using a 150-ms mixing time with hypercomplex phase cycling and 512 complex points in the t_1 dimension.

RESULTS

Biochemical Characterization of Recombinant Human Prothymosin α. Two techniques, SDS−PAGE and UV absorption, were applied to check the purity of the isolated ProTα. SDS−PAGE analysis shows the existence of only one band in the lane of the isolated product. The band corresponds to a protein with molecular mass (M_r) of ∼13 kDa (see inset to Figure 1). This value is close the molecular mass of ProTα calculated from the amino acid sequence (12.21 kDa). Figure 1 shows that the absorption spectrum of the purified protein is an unusual one with no absorption bands in the vicinity of 260−280 nm. However, such behavior was expected for ProTα as this protein has no aromatic amino acid residues.

It was already noted that ProTα might be associated with cell proliferation. To test the activity of the isolated protein, its capability to stimulate thymocyte proliferation was studied

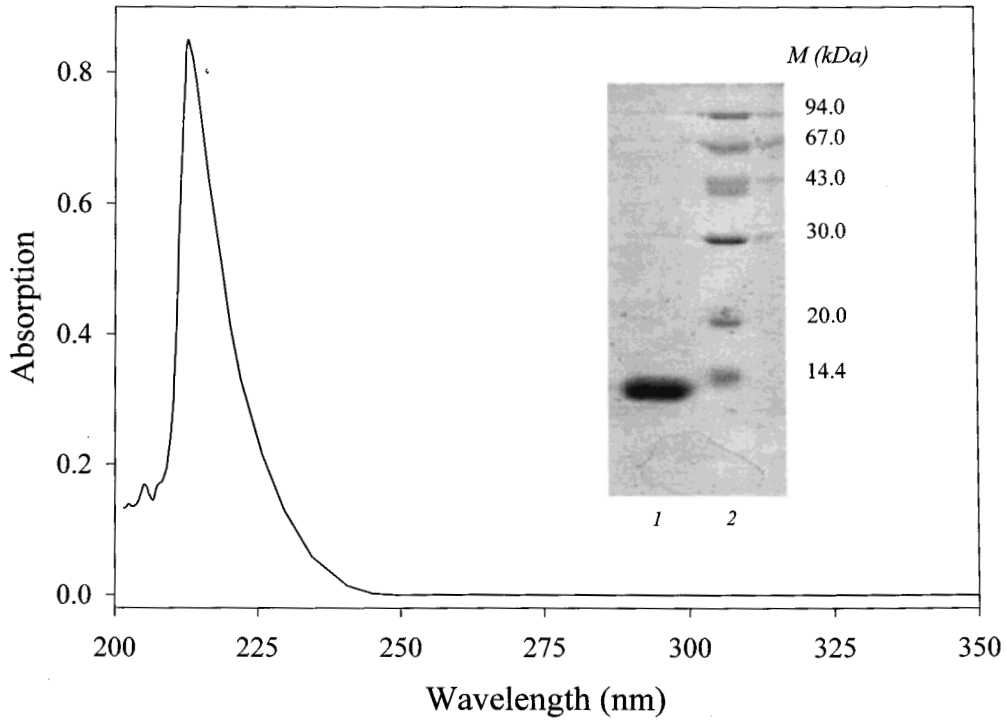

FIGURE 1: Purity of the isolated recombinant human prothymosin α. UV absorption spectrum and SDS−PAGE (inset) of the protein. Electrophoresis was carried out using 12% polyacrylamide gel as described in ref *34*. The gel was stained with Coomassie Brilliant Blue R-250 (Pharmacia), washed off, and dried. Slot 1, purified human ProTα; slot 2, molecular mass markers (Pharmacia); M, molecular mass of proteins−markers (in kDa). Cell path length for the absorption measurements was 10 mm.

Table 1: ProTα- and Interleukin-4-Induced Stimulation of Human Thymocytes Proliferation

protein (concn)	no. of counts per min	stimulation index	sample treatment
ProTα (10^{-9} M)	46800 ± 3200	2.0	without heating
	50600 ± 4800	2.4	incubated for 30 min at 56 °C
	48500 ± 3600	2.3	incubated three times for 30 min at 56 °C with 20-min incubation at 25 °C between
	44700 ± 2200	2.2	incubated three times for 5 min at 80 °C, with 30-min incubation at 25 °C between
	50100 ± 6000	2.4	incubated four times for 5 min at 80 °C, with 30-min incubation at 25 °C between
	47600 ± 4300	2.3	incubated for 10 min at 100 °C
control	20700 ± 1700	1.0	thymocytes + Con A (2 μg/mL)
rHuIL-4 (10^{-9} M)	31700 ± 2700	2.1	without heating
	16100 ± 1600	1.1	incubated for 30 min at 56 °C
control	15300 ± 1500	1.0	thymocytes + Con A (1 μg/mL)

(*33*, *35*). It has been established that ProTα promotes the mitogen-induced proliferation of human thymocytes. This effect reaches saturation at doses of ProTα ranging from 10^{-7} to 10^{-9} M. Interestingly, the value of the stimulation index was virtually independent of sample heating. The results of such investigations are summarized in Table 1. Quite different results are observed for human interleukin-4, which is also capable of increasing the Con A-induced proliferation of T cells (*43*): Table 1 shows that the stimulation activity of this protein is almost completely suppressed by a 30-min incubation at 56 °C. In contrast, such heating had no effect on the activity of ProTα. These observations can be explained by taking into account the structural difference between the two proteins at physiological conditions. rHuIL-4 is a normal globular protein with a rigid, tertiary structure, as seen by X-ray crystallography (*44*), and becomes denatured at 56 °C; on the other hand, ProTα has no ordered structure even at 25 °C (*16*, *18*) and, thus, cannot be unfolded by further increase in temperature.

Acidification of Solution Induces Structural Changes in the Unfolded ProTα Molecule. The inset to Figure 2 shows that at pH 7.5 ProTα is characterized by a far-UV CD spectrum, which is typical of unfolded proteins, but at pH 2.5 a considerable rearrangement of the spectrum is observed. In particular, the position of the major minimum is shifted to a higher wavelength, and a pronounced decrease of the trough at 200 nm is observed accompanied by a considerable increase in ellipticity at 222 nm. Such far-UV CD spectral changes can be explained by the appearance of some α-helix in the protein at low pH (*45*, *46*). Our data are consistent with the assumption that a decrease of pH from pH 7.5 to pH 2.5 is accompanied by an increase in the helical content from 0% to ∼15%. The data at pH 7.5 are in good agreement with the results of previous investigations, where it was established that ProTα at neutral pH adopts a random coil conformation (*16*, *18*, *19*).

The process of pH-induced secondary structure formation in ProTα is visualized in Figure 2 as $[\theta]_{222}$ vs pH dependence. It can be seen that the protein far-UV CD spectrum is unchanged between pH ∼9.5 and pH ∼5.5; however, the decrease in pH from 5.5 to 3.5 results in a ∼5-fold increase in intensity of the spectrum, while a further decrease in pH

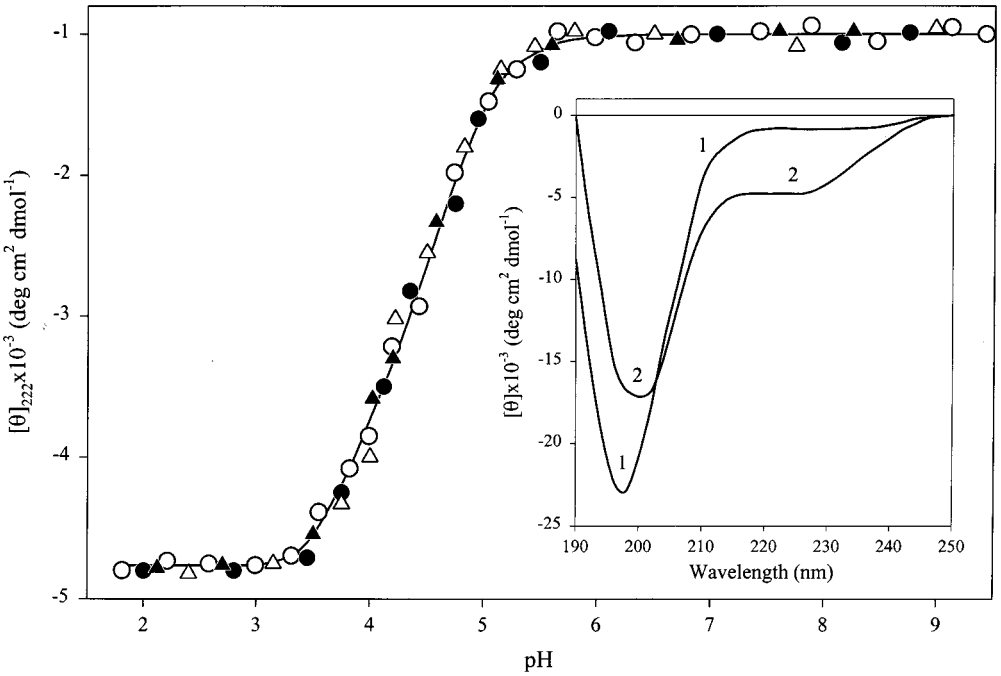

FIGURE 2: pH-induced changes in ProTα far-UV CD spectra monitored as the pH dependence of the $[\theta]_{222}$ value. Inset represents spectra of the protein at pH 7.5 and pH 2.5 (marked as 1 and 2, respectively). Measurements were carried out at 20 °C. Protein concentration was 0.6 (circles) and 2.5 mg/mL (triangles). Results of direct (decrease in pH value) and back experiments (increase in pH value) are presented as open and solid symbols, respectively. Cell path length was 0.148 mm.

is not accompanied by spectral changes. Figure 2 shows that the pH-induced changes in the far-UV CD spectrum of ProTα are completely reversible (compare open and solid symbols) and are independent of protein concentration (at least in the range of 0.6−2.5 mg/mL, compare circles and triangles). These observations are consistent with the assumption that the increase in structure of ProTα represents an intramolecular process and not association.

Changes in ANS fluorescence are frequently used to detect nonnative, intermediate conformations of globular proteins (*31*, *47*, *48*). This is because such intermediates are characterized by the presence of solvent-exposed hydrophobic clusters, resulting in a considerable increase in the ANS fluorescence intensity and in a pronounced blue shift of the fluorescence emission maximum (*47*, *48*). The inset to Figure 3 shows that in the case of ProTα a decrease in pH leads to considerable changes in ANS fluorescence (compare curves 1 and 2), reflecting the pH-induced transformation to the partially folded compact conformation. The formation of this intermediate is reflected in the pH dependence of the ANS fluorescence intensity (see Figure 3). The pH dependence of free ANS is also presented for comparison. It follows from Figure 3 that the transition from unfolded to partially folded conformation takes place between pH 5.5 and pH 3.5. It also can be seen that the pH-induced structural changes are completely reversible (Figure 3, open and solid symbols).

Figure 4 compares the results of ANS fluorescence and CD measurements. It is seen that these parameters change simultaneously in a rather cooperative manner. This means that acidification of ProTα solution results in transformation of the random coil ProTα into a conformation with significant secondary structure and with affinity for ANS. Our further investigations were devoted to the structural characterization of this conformation.

Structural Characteristics and Conformational Stability of ProTα at Low pH Values. (a) Hydrodynamic Investigations by Gel Filtration. To obtain information on pH-induced changes of the ProTα hydrodynamic dimensions, the gel filtration behavior of the protein under different experimental conditions was studied. The gel permeation column separates proteins by differences in their hydrodynamic dimensions rather than by their molecular mass (*39*). This approach can be successfully applied to determine the Stokes radius values for a protein in different conformational states (*36*, *37*, *40*). We have studied ProTα by size exclusion chromatography at neutral and acid pH and in the presence of 8 M urea. In all cases, the gel filtration profile contained a single symmetric elution peak. The position of this peak was used to calculate the R_S value (see Materials and Methods). The results of chromatographic analysis are presented in Table 2. It is evident that the hydrodynamic dimensions of ProTα at neutral pH are close to those measured in the presence of 8 M urea. The small difference between the two values is due to swelling of the unfolded polypeptide chain in a good solvent (*20*). Both values are virtually indistinguishable from R_S, calculated for the completely unfolded protein with a molecular mass of 12.21 kDa. Table 2 shows that a decrease in pH leads to a pronounced decrease of the ProTα hydrodynamic dimension. It should be emphasized that the R_S value determined for ProTα at pH 2.5 is still far from that expected for a globular protein of 12 kDa.

(b) SAXS Data. Small-angle X-ray scattering (SAXS) represents a powerful tool in the investigation of conformation, shape, and dimensions of biopolymer molecules in solution. Analysis of the scattering curves using the Guinier approximation gives information about the R_g values for different experimental conditions. Presentation of the scattering data in the form of Kratky plots provides information about the globularity and conformation of a protein (*49*).

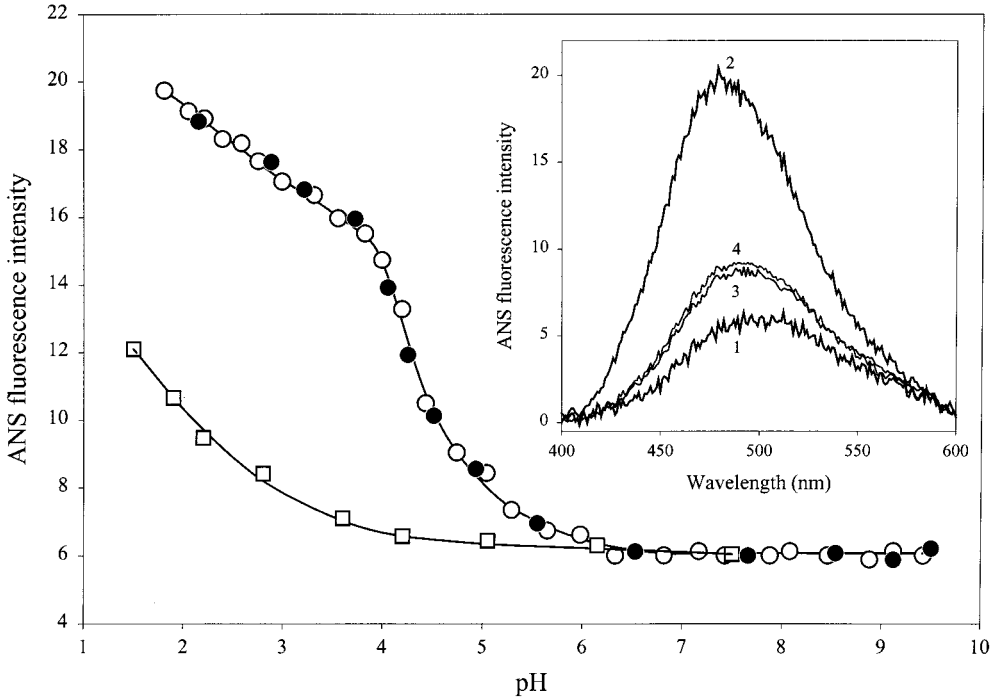

FIGURE 3: pH-induced changes of ANS fluorescence intensity in ProTα-containing solutions. Protein concentration was 0.1 mg/mL. ANS concentration was 25 μM. Results of direct (decrease in pH value) and back experiments (increase in pH value) are shown by open and solid symbols, respectively. pH dependence of free ANS fluorescence intensity is shown by open squares. Inset represents spectra of ANS in the presence of ProTα measured at pH 7.5 and pH 2.5 (marked as 1 and 2, respectively). Spectrum of free ANS at pH 2.5 (curve 3) and that of the dye in the presence of polyglutamic acid in α-helical conformation (pH 2.5, curve 4) are shown for comparison. Fluorescence was excited at 360 nm. Measurements were carried out at 20 °C.

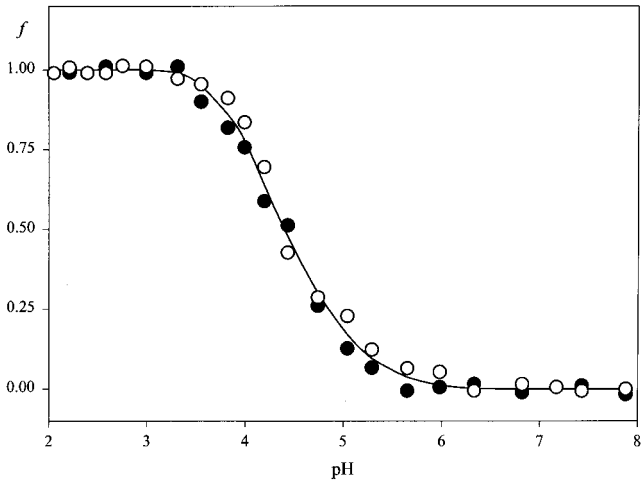

FIGURE 4: Comparison of the pH effect on ProTα far-UV CD spectra and the capability of protein to interact with ANS. Plot represents the normalized $[\theta]_{222}$ vs pH (solid circles) and I^{ANS} vs pH (open circles) dependence.

Table 2: Hydrodynamic Dimensions of ProTα under Different Experimental Conditions

conformation, conditions	V^{el} (mL)	R_S (Å)	R_S^U/R_S	R_S/R_S^N
random coil, pH 7.5	13.35 ± 0.08	31.4 ± 0.3	1.04	1.76
random coil, pH 7.5, 8 M urea	13.17 ± 0.08	32.8 ± 0.3	1.00	1.84
partially folded, pH 2.2	14.25 ± 0.08	24.9 ± 0.3	1.29	1.40
N (calculated)[a]		17.9	1.75	1.00
MG (calculated)[a]		20.6	1.52	1.15
U (calculated)[a]		31.3	1.00	1.75

[a] The R_S values for the native and completely unfolded by 8 M urea protein of 12.21 kDa (see lines N and U) were calculated as described in ref *36*, using the equations: $\log (R_S^N) = 0.369 \log (M) - 0.254$ and $\log (R_S^U) = 0.533 \log (M) - 0.682$, respectively. R_S for the "classical" molten globule state was calculated from the corresponding native value, assuming a 1.15-fold increase over the native value (*31*).

For a native globular protein this plot has a characteristic maximum, whereas unfolded and partially folded polypeptides have significantly different shaped Kratky plots.

Guinier analysis of scattering data shows that at neutral pH ProTα is characterized by an R_g of 37.8 ± 0.9 Å, which is somewhat lower than previously reported (*18*). At low pH this parameter decreases to 27.6 ± 0.8, reflecting considerable compaction of the protein molecule (the volume decreases 2.5-fold). Analysis of the X-ray scattering in the form of a Kratky plot shows that ProTα does not have well-developed globular structure under any condition studied (Figure 5). The profile of the Kratky plot at neutral pH is typical for a random coil conformation, whereas at pH 2.5 considerable change in the shape of the scattering curves is detected, reflecting the presence of more ordered conformation under such conditions.

(c) ^{1}H NMR. Proton NMR spectra were collected to ascertain whether prothymosin undergoes significant structural changes as a function of pH. As shown in Figure 6A, the ^{1}H NMR spectrum of prothymosin at pH 8.0 was characteristic of a highly denatured protein. The resonances were sharp (indicating a high degree of rapid local segmental motion), the amide proton resonances were weak in intensity (indicating little regular hydrogen bonding due to hydrogen exchange with bulk solvent), and the spectrum was poorly dispersed. At pH 2.4 (Figure 6B), prothymosin still gave a spectrum characteristic of a denatured protein, although significant differences were observed as compared to pH 8.5. These differences included changes in the chemical shifts of some carbon-attached protons (which, being nonexchange-

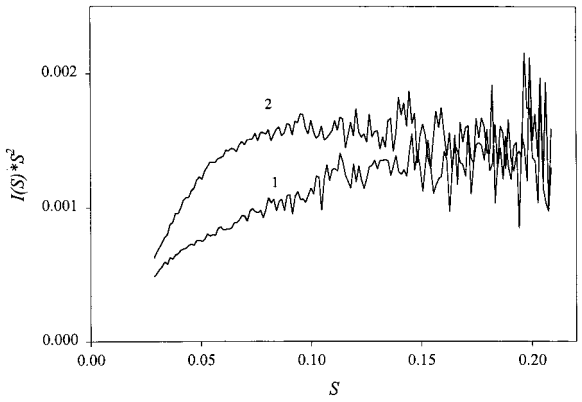

FIGURE 5: Kratky plot representation of the results of small-angle X-ray scattering analysis of ProTα at different experimental conditions: 1, pH 7.5; 2, pH 2.5. Measurements were carried out at 25 °C. Protein concentration was 0.95 mg/mL.

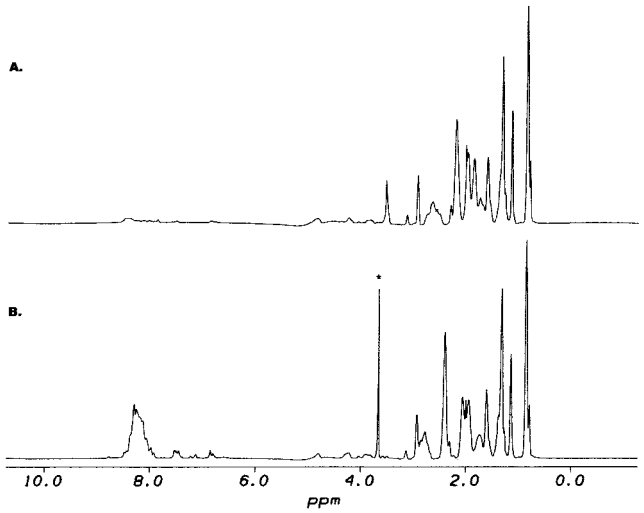

FIGURE 6: ^{1}H NMR spectra of prothymosin α at pH 8.0 (A) and pH 2.4 (B). The peak denoted with an asterisk is from residual buffer present in the lyophilized protein.

able, should not be dependent on the pH of the bulk solvent) and an increase in the line widths of some aliphatic resonances. These observations strongly suggest that a structural change had occurred, with the polypeptide becoming more compact and ordered.

To further characterize the structural changes that occurred in prothymosin at pH 2.8, NOESY spectra were collected to look for through-space interactions between protons. Unfortunately, no apparent long-range NOE cross-peaks were observed in the spectrum at pH 2.8, suggesting that the structure of prothymosin at low pH is undergoing rapid conformational exchange.

(d) Urea-Induced Unfolding. Urea- or GdmCl-induced unfolding is frequently used for probing protein stability under equilibrium conditions. The results of such investigations for the acid conformation of ProTα are represented in Figure 7. One can see that the urea-induced unfolding of the ProTα acid conformation is a completely reversible process. Parameters of the ProTα unfolding−refolding are independent of protein concentration, indicating that aggregation is absent. Figure 7 shows that the denaturant-induced unfolding of the ProTα acid state represents a very broad transition characterized by the absence of the sigmoid shape, typical of the unfolding of native and molten globule

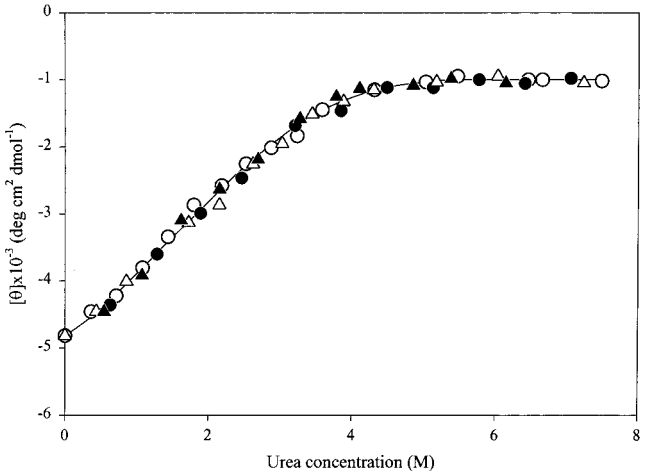

FIGURE 7: Urea-induced unfolding of the ProTα acid form monitored by the changes in far-UV CD spectrum intensity. Protein concentration was 0.6 (circles) and 2.5 mg/mL (triangles). Open and solid symbols correspond to the unfolding and refolding experiments, respectively. Cell path length was 0.148 mm. Measurements were carried out at 20 °C.

conformations (*50, 51*). Similar behavior was reported for denaturant-induced unfolding of the premolten globule state of proteins such as carbonic anhydrase, β-lactamase, and staphylococcal nuclease (*20*−*29*).

DISCUSSION

Low pH Conformation of ProTα: Compact Denatured State of the Protein or Helical Form of Polyglutamic Acid? The results presented in this paper demonstrate that at neutral pH the recombinant human prothymosin α possesses all the properties of the unfolded state, whereas lowering the pH results in the transformation of the protein into a partially folded conformation. At pH 7.5, ProTα has no regular secondary structure, and its hydrodynamic dimensions are typical of a random coil with a molecular mass of ∼12 kDa. Furthermore, it does not interact with the fluorescent probe ANS, suggesting few hydrophobic surface patches or pockets.

The existence of a cooperative structural transition in the pH range of 5.5−3.5, separating the unfolded ProTα (at neutral pH) from a partially folded conformation (at low pH), has been established. This is a sigmoidal transition with a half-transition point at about pH 4.4, as measured by changes in the far-UV CD and ANS fluorescence spectra. The pH-induced changes of ProTα were highly reversible and independent of protein concentration, with no detectable pH-induced association of the protein. In other words, we can assume that the observed changes are of an intra- rather than an intermolecular character.

The acid state of ProTα, populated below pH 3.5, shows characteristics of being partially folded. These include the enhancement of ANS fluorescence, an increase in helicity measured by CD, and partial compaction as R_S and R_g values are ∼1.3-fold smaller than those of the random coil conformation.

Proton NMR spectra were collected to further characterize the structural changes that occur in prothymosin under acidic conditions. Analysis of these spectra showed that significant structural differences did occur on changing the pH of the protein from 8.0 to 2.4. These changes, however, did not represent the formation of a tightly packed globular structure but were consistent with the collapse of the chain into a more

compact denatured state than that at pH 8.0. This was further supported by the lack of any long-range NOEs, indicating that little regular secondary structure was formed. In this light, the increase in helicity observed in the low pH CD spectra of prothymosin is likely due to the transient population of secondary structure. This matter will be further investigated on complete assignment of the prothymosin NMR spectrum by measuring the chemical shift index for Hα and Cα resonances, which has the potential for providing an estimate of the fractional population of regular secondary structures in compact denatured states of proteins.

The question then arises as to nature of the low pH conformation. There are two possible answers to this question. Due to the high Glu content in ProTα, the decrease in pH may lead to the formation of independent polyglutamic acid-like α-helices. On the other hand, the increased helicity induced at low pH may be associated with the appearance of a partially folded conformation or compact denatured state. To address this problem, the binding of ANS by ProTα was investigated. It was already noted that changes in the fluorescence parameters of this hydrophobic dye represent a useful tool in monitoring the formation of partially folded conformations of proteins (*31, 47, 48*). The inset to Figure 3 shows that, in the presence of the low pH conformation of ProTα, the ANS fluorescence undergoes considerable intensity change and is blue-shifted. One can argue that these changes might be explained by the protonation of ANS. Indeed, the latter can lead either to changes in the spectral properties of ANS itself or to higher affinity of the protonated dye to the polypeptide chain (i.e., the pH dependence of the ANS fluorescence parameters may have nothing to do with conformational changes of the protein). To account for such a possibility, the inset to Figure 3 represents spectra measured for free ANS at pH 2.5 and for the dye in the presence of polyglutamic acid in α-helical conformation (curves 3 and 4, respectively). Whereas the fluorescence of free ANS is affected by the decrease in pH, formation of helical structure in polyglutamic acid is not accompanied by any ANS spectral changes, reflecting the absence of ANS−polyglutamate complexes. Both these findings are in good agreement with earlier observations (*48*). However, the inset to Figure 3 shows that the largest changes of the ANS fluorescence parameters are observed in the presence of the low pH conformation of ProTα.

It has been established that ANS binding to a polypeptide chain is primarily determined by the formation of ion pairs between ANS^- anion (the sulfonate SO_3^- group) and the cationic groups (lysine, arginine, and histidine side chains) of a protein (*52*). Interestingly, the formation of stable ANS−protein complexes is not sufficient for the enhancement of the dye fluorescence. Indeed, among ∼90 ANS^- anions strongly bound to a BSA molecule at pH below 5.0, only five show strong fluorescence, whereas the majority of the bound dye is not fluorescent (*52*). It has been also shown that free ANS in aqueous solutions is not fluorescent, whereas it has strong emission in nonpolar organic solvents (*53*−*55*), suggesting that the changes of ANS fluorescent properties are mainly due to the changes in polarity of the dye microenvironment. On the other hand, the absence of ANS spectral changes in the presence of unfolded proteins (where each hydrophobic residue is accessible to the solvent) indicates that the contact of the dye with the *individual* hydrophobic groups does not furnish the necessary environment (*48, 56*). However, such a microenvironment can be created by assembly of the individual hydrophobic groups into solvent accessible hydrophobic clusters or patches, which is a characteristic feature of partially folded protein (*31, 47, 48, 56*). Thus, the presence of pronounced changes in the ANS fluorescence is consistent with the assumption that in the case of ProTα at low pH we are dealing with the formation of an intermediate state characterized by the existence of hydrophobic clusters exposed to the solvent.

Data on SAXS from the solution of the ProTα acid form gives an additional confirmation of this suggestion. It has been established that the formation of α-helical conformation in the homopolymer polylysine is not accompanied by any changes in the shape of the Kratky plot (*49*). In contrast, Figure 5 shows that acidification of the ProTα solution leads to pronounced alterations in the shape of the Kratky plot.

In conclusion, the data presented in this paper suggest that at low pH ProTα is in a collapsed partially folded conformation with relatively developed secondary structure and characterized by the presence of solvent accessible hydrophobic clusters. The mechanism of the pH-induced folding of ProTα can be easily understood using simple analysis of its amino acid sequence. The net charge of ProTα at neutral pH can be as high as −44. This means that a decrease in pH leads to neutralization of the negatively charged acidic residues. Formation of α-helical structure by the glutamic acid-rich regions of the protein might be expected (*16, 18*), which, in turn, might be accompanied by the hydrophobic collapse of at least part of the ProTα molecule.

It has been shown that globular proteins can populate at least two relatively compact partially folded conformations: the molten globule and premolten globule states (*20*−*29*). The structural properties of the molten globule have been summarized in a number of reviews (e.g., ref *31*). The structural peculiarities of a polypeptide chain in the premolten globule state are summarized below. The protein in this state is denatured, having no rigid tertiary structure. It contains substantial secondary structure, although much less than that of the native or the molten globule protein (∼50% native secondary structure vs ∼100% in the molten globule state). The hydrodynamic volume of a protein in the molten globule, the premolten globule, and the unfolded states is respectively 1.5, ∼3, and ∼12 times larger than that of the native state. The protein in the premolten globule state can effectively interact with the hydrophobic fluorescent probe ANS, though the interaction is weaker than in the molten globule state. Finally, premolten globule states do not have specific globular structure, as indicated by Kratky analysis of the SAXS data.

On the basis of these observations, we conclude that ProTα in the acid form possesses all the properties of the premolten globule. It is possible that the same conformational transitions can take place in vivo and thus may be associated with the activity of this interesting protein. It is known that the 3D structure of a protein may be maintained by interactions with specific ligands (*57*). Taking into account this fact, it is difficult to exclude the possibility that ProTα may have ordered secondary structure even at neutral pH due to interaction with specific ligands, e.g., metal ions, nucleic acid, or other proteins. To confirm this idea, we have analyzed the structure-forming effect of several bivalent cations. In

agreement with Gast et al. (*18*), it was established that ProTα conformation is unaffected by large excess of Ca^{2+} and Mg^{2+}. However, Zn^{2+} induces substantial secondary structure in ProTα at neutral pH. Interestingly, the effect of this cation on the ProTα far-UV CD spectrum was identical to that of acidic pH (Uversky, unpublished data). This means that ProTα can interact with Zn^{2+} ($K_D \sim 10^{-3}$ M), and that such interactions induce partial folding of the unfolded protein molecule at neutral pH. As acidic amino acids may form specific metal binding centers in proteins (*58*), we assume that the Glu/Asp-rich part of the ProTα molecule is responsible for the formation of the Zn^{2+}-binding sites. Further investigations are required to clarify this suggestion.

ACKNOWLEDGMENT

The authors express their gratitude to V. P. Zav'yalov for valuable discussions of the results and to A. V. Vartapetyan for the kind gift of *E.coli* line, overproducing prothymosin α.

REFERENCES

1. Haritos, A. A., Tsolas, O., and Horecker, B. L. (1984) *Proc. Natl. Acad. Sci. U.S.A. 81*, 1391−1393.
2. Economou, M., Seferiadis, K., Frangou-Lazaridis, M., Horecker, B. L., and Tsolas, O. (1988) *FEBS Lett. 233*, 342−346.
3. Haritos, A. A., Goodall, G. A., and Horecker, B. L. (1984) *Proc. Natl. Acad. Sci. U.S.A. 81*, 1008−1011.
4. Clinton, M., Frangou-Lazaridis, M., Paneerselvam, C., and Horecker, B. L. (1989) *Arch. Biochem. Biophys. 269*, 256−263.
5. Goldstein, A. L., Low, T. L., Thurman, G. B., Zatz, M. M., Hall, N., Chen, J., Hu, S. K., Naylor, P. B., and McClure, J. E. (1981) *Recent Prog. Horm. Res. 37*, 369−415.
6. Goldstein, A. L., Zatz, M. M., Low, T. L., and Jacobs, R. (1981) *Ann. N. Y. Acad. Sci. 377*, 486-495.
7. Naylor, P. H., Low, T. L. K., and Goldstein, A. L. (1984) *Bioassays 63*, 80−87.
8. Haritos, A. A., Salvin, S. B., Blacher, R., Stein, S., and Horecker, B. L. (1985) *Proc. Natl. Acad. Sci. U.S.A. 82*, 1050−1053.
9. Baxevanis, C. N., Reclos, G. J., Economou, M., Arsenis, P., Katsiyiannis, A., Seferiades, K., Papadopoulos, G., Tsolas, O., and Papamichail, M. (1988) *Immunopharmacol. Immunotoxicol. 10*, 443−461.
10. Baxevanis, C. N., Frillingos, S., Seferiadis, K., Reclos, G. J., Arsenis, P., Katsiyiannis, A., Anastasopoulos, E., Tsolas, O., and Papamichail, M. (1990) *Immunopharmacol. Immunotoxicol. 12*, 595−617.
11. Papanastasiou, M., Baxevanis, C. N., and Papamichail, M. (1992) *Cancer Immunol. Immunother. 35*, 145−150.
12. Eilers, M., Schirm, S., and Bishop, J. M. (1991) *EMBO J. 10*, 133−141.
13. Tsitsiloni, O. E., Stiakakis, J., Koutselinis, A., Gogas, J., Markopoulos, Ch., Yialouris, P., Bekris, S., Panoussopulos, D., Kiortsis, V., Voelter, W., and Haritos, A. A. (1993) *Proc. Natl. Acad. Sci. U.S.A. 90*, 9504−9507.
14. Sburlati, A. R., Manrow, R. E., and Berger, S. L. (1991) *Proc. Natl. Acad. Sci. U.S.A. 88*, 253−257.
15. Manrow, R. E., Sburlati, A. R., Hanover, J. A., and Berger, S. L. (1991) *J. Biol. Chem. 266*, 3916−3924.
16. Watts, J. D., Cary, P. D., Sautiere, P., and Crane-Robinson, C. (1990) *Eur. J. Biochem. 192*, 643−651.
17. Papamarcaki, T., and Tsolas, O. (1994) *FEBS Lett. 345*, 71−75.
18. Gast, K., Damashun, H., Eckert, K., Schultze-Forster, K., Maurer, R., Müller-Frohne, M., Zirwer, D., Czarnecki, J., and Damashun, G. (1995) *Biochemistry 34*, 13211−13218.
19. Cordero, O. J., Sarandese, C. S., Lopez, J. L., and Nogueira, M. (1992) *Biochem. Int. 28*, 1117−1124.
20. Uversky, V. N., and Ptitsyn, O. B. (1994) *Biochemistry 33*, 2782−2791.
21. Uversky, V. N., and Ptitsyn, O. B. (1996) *J. Mol. Biol. 255*, 215−228.
22. Uversky, V. N., and Ptitsyn, O. B. (1996) *Mol. Biol. (Moscow) 30*, 672−678.
23. Uversky, V. N., and Ptitsyn, O. B. (1996) *Mol. Biol. (Moscow) 30*, 679−684.
24. Ptitsyn, O. B., Bychkova, V. E., and Uversky, V. N. (1995) *Philos. Trans. R. Soc. London B 348*, 35−41.
25. Uversky, V. N. (1998) *Protein Pept. Lett. 4*, 355−367.
26. Uversky, V. N. (1998) *Biophysics (Moscow) 43*, 416−421.
27. Uversky, V. N. (1998) *Mol. Biol. (Moscow) 32*, 473−478.
28. Uversky, V. N. (1998) *Mol. Biol. (Moscow) 32*, 479−488.
29. Uversky, V. N., Karnoup, A. S., Segel, D. J., Seshadri, S., Doniach, S., and Fink, A. L. (1998) *J. Mol. Biol. 278*, 879−894.
30. Bychkova, V. E., Pain, R. H., and Ptitsyn, O. B. (1988) *FEBS Lett. 238*, 231−234.
31. Ptitsyn, O. B. (1995) *Adv. Protein Chem. 47*, 83−229.
32. Bychkova, V. E., and Ptitsyn O. B. (1993) *Chemtracts: Biochem. Mol. Biol. 4*, 133−163.
33. Evstafieva, A. G., Chichkova, N. V., Makarova, T. N., Vartapetian, A. B., Vasilenko, A. V., Abramov, V. M., and Bogdanov, A. A. (1995) *Eur. J. Biochem. 231*, 639−643.
34. Laemmli, U. (1970) *Nature 227*, 680−685.
35. Janossy, G. M., Greaves, F., Doenholf, M. J., and Snajder, J. (1973) *Clin. Exp. Immunol. 14*, 581−586.
36. Uversky, V. N. (1993) *Biochemistry 32*, 13288−13298.
37. Uversky, V. N. (1994) *Int. J. Bio-Chem. 1*, 103−114.
38. Ackers, G. L. (1967) *J. Biol. Chem. 242*, 3237−3238.
39. Ackers, G. L. (1970) *Adv. Protein Chem. 24*, 343−446.
40. Corbett, R. J., and Roche, R. S. (1984) *Biochemistry 23*, 1888−1894.
41. Tanford, C. (1968) *Adv. Protein Chem. 23*, 121−282.
42. Glatter, O., and Kratky, O. (1982) *Small-angle X-ray scattering*, Academic Press, New York.
43. Rybak, M. E. (1994) in *The Cytokine*, 2nd ed. (Thomson, A., Ed.) p 99, Academic Press, New York.
44. Wlodawer, A., Pavlovsky, A., and Gustchina A. (1992) *FEBS Lett. 309*, 59−64.
45. Chen, Y.-H., Yang, J. T., and Chau, K. H. (1974) *Biochemistry 13*, 3350−3359.
46. Chou, P. Y., and Fasman, G. D. (1974) *Biochemistry 13*, 222−245.
47. Rodionova, N. A., Semisotnov, G. V., Kutyshenko, V. P., Uversky, V. N., Bolotina, I. A., Bychkova, V. E., and Ptitsyn, O. B. (1989) *Mol. Biol. (Moscow) 23*, 683−692.
48. Semisotnov, G. V., Rodionova, N. V., Razgulyaev, O. I., Uversky, V. N., Gripas, A. F., and Gilmanshin, R. I. (1991) *Biopolymers 31*, 119−128.
49. Semisotnov, G. V., Kihara, H., Kotova, N. V., Kimura, K., Amemiya, Y., Wakabayashi, K., Serdyuk, I. N., Timchenko, A. A., Chiba, K., Nikaido, K., Ikura, T., and Kuwajima, K. (1996) *J. Mol. Biol. 262*, 559−574.
50. Ptitsyn, O. B., and Uversky, V. N. (1994) *FEBS Lett. 341*, 15−18.
51. Uversky, V. N., and Ptitsyn, O. B. (1996) *Folding Des. 1*, 117−122.
52. Matilus, D., and Lovrien, R. (1998) *Biophys. J. 74*, 422−429.
53. Strier, L. (1965) *J. Mol. Biol. 13*, 482−495.
54. Slavik, J. (1982) *Biochim. Biophys. Acta 694*, 1−25.
55. Uversky, V. N., Winter, S., and Löber, G. (1998) *Biochim. Biophys. Acta 1388*, 133−142.
56. Uversky, V. N., Winter, S., and Löber, G. (1996) *Biophys. Chem. 60*, 79−88.
57. Uversky, V. N., and Narizhneva, N. V. (1998) *Biochemistry (Moscow) 63*, 420−433.
58. Chakrabarti, P. (1990) *Protein Eng. 4*, 49−50.

BI990752+